

## <sup>13</sup>C NMR INVESTIGATIONS OF THE STRUCTURE IN SOLID POLYMERS

G. Hempel and H. Schneider

Department of Physics, Technical University "Carl Schorlemmer",  
4200 Merseburg, GDR

**Abstract** - Cross-polarization <sup>13</sup>C NMR spectroscopy was applied to get information about the structure in isotropic and oriented solid polymers. From the variation of the line shape caused by the stretching of the sample have been calculated mean orientations in highly oriented fibres (polyimide) and orientation distributions of chain segments in a weakly oriented polymer (polycarbonate). Shielding tensor component distributions obtained numerically from the spectra were compared with the degree of crystallinity and were used to distinguish regions of different order (polycarbonate) and to study the abundance of various conformations (polyethylene).

### I. INTRODUCTION

Since the publication of the basic work of Pines, Gibby, and Waugh in 1973, the measurement of highly resolved NMR spectra in solids has become possible also for rare spins (Ref. 1). Using the cross-polarization of the <sup>13</sup>C nuclei via the protons and decoupling these during the observation of the free induction decay, one gets (after the Fourier transform) spectra without dipolar broadening of the lines. [In comparison with the usual measured <sup>13</sup>C spectra after a  $\pi/2$ -pulse and with proton-decoupling, the main advantage is a better signal-to-noise ratio arising from a higher <sup>13</sup>C magnetization by means of the cross-polarization by a factor of about two (theoretically four) and from the fact that the longitudinal relaxation function  $T_1$  of the protons instead of the much larger one of the <sup>13</sup>C nuclei determines the repetition rate of the experiments.]

However, the anisotropy of chemical shift fully influences the line shape and often yields an overlapping of several lines. Averaging out this effect by magic-angle spinning (MAS) allows to separate different lines. Unfortunately, this is connected with a loss of information, and the anisotropy of shielding tensor plays an important role in our treatment. Therefore, it is necessary to use a small deviation of the magic angle in order to observe separated lines with a not fully reduced anisotropy of the chemical shielding. The spectra discussed here were obtained without MAS. The application of the cross-polarization technique (CP) to the investigation of solid polymers generally yields spectra which differ from the line shapes characteristic of polycrystalline samples by smoothing of these lines as a result of a distribution of shielding tensor elements in polymers. Consequently, relatively structureless lines occur in the spectrum. The question arises, if it is possible to get some information about the amorphous materials from these smoothed lines, e.g. the degree of smoothing in connection with the amorphousness, or the distribution of tensor elements in relation to a distribution of structural parameters. This question will be discussed in section III.

Another reason for a variation of the line shape in polymer spectra may be unequally distributed orientation probabilities in the stretched polymers. Again the above-mentioned question arises which is discussed in section II.

The experimental work was done by using a Bruker SXP 4-100 spectrometer with a high-power proton-decoupling unit. The Larmor-frequency and the magnetic radio-frequency field for the <sup>13</sup>C-nuclei were 22.64 MHz and 4 mT, respectively.

### II. ORIENTED POLYMERS

If the molecules are oriented in the sample, the line shape must be changed in a characteristic way determined by an orientation distribution function. This implies the possibility of obtaining the latter from the NMR spectrum using a quantitative relation between it and the line shape function. Thus, such a relation has to be derived (see part II. A.).

In the case of polymers with very strong orientation, e.g. in fibres, it is of great importance to gain knowledge of the orientation of the various atom groups or chain segments relative to the draw direction. Often this problem is easily solved by X-ray scattering, but in some cases this method cannot yield the whole information wanted. The solid state NMR spectrum is very sensitive to an anisotropy of the sample because of the orientation dependence of the chemical shift. This can be used to get structural data not available from other methods (see part II. B.).

#### A. LINE SHAPE

The chemical shift is a second rank tensor  $\vec{\sigma}$ . The principal axes ( $x_1, x_2, x_3$ ) of  $\vec{\sigma}$  are related to the laboratory frame ( $x, y, z$ ) (the magnetic field  $\vec{H}_0$  is aligned parallel to the  $z$ -direction) by the Euler angles  $\phi, \theta, \psi$ , and the observed shift  $\sigma = \sigma_{zz}$  is given by

$$\sigma = \sin^2\theta \cos^2\phi \sigma_{11} + \sin^2\theta \sin^2\phi \sigma_{22} + \cos^2\theta \sigma_{33} \quad (1)$$

For the case of uniaxial symmetry yields with  $\sigma_{11} = \sigma_{\parallel}$ ,  $\sigma_{22} = \sigma_{33} = \sigma_{\perp}$

$$\sigma = \sigma_{\parallel} \cos^2\theta + \sigma_{\perp} \sin^2\theta \quad (2)$$

The line shape  $G(\sigma)$  follows from the distribution function  $f(\cos\theta)$  according to

$$G(\sigma) d\sigma = f(\cos\theta) d(\cos\theta). \quad (3)$$

In an isotropic sample the  $(\cos\theta)$ -values are equally distributed, and eqn. (3) gives

$$G_0(\sigma) = d(\cos\theta)/d\sigma \quad (4)$$

with regard to eqn. (2). Therefore, for anisotropic materials with a distribution of  $(\cos\theta)$  the line shape is given by

$$G(\sigma) = f(\cos\theta) G_0(\sigma). \quad (5)$$

Examples of line shapes for different distribution functions  $f(\cos\theta)$  according to eqn. (5) are given in Fig. 1.

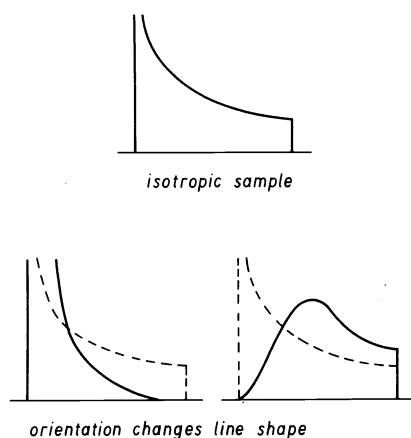


Fig. 1. The change of the line shape because of the orientation

#### B. STRONG ORIENTATION

In polymers with a strong orientation, e.g. in fibres, we want to estimate an averaged value for the inclination  $\gamma$  between the orientation of the segments ( $\vec{S}$ ) and the draw-direction ( $\vec{V}$ ) using the angle  $\beta$  between the draw-direction and the principal axis which relates to the eigenvalue  $\sigma_{11}$ . If  $\vec{V}$  is parallel in respect to  $\vec{B}_0$ , one gets a single narrow line on the position

$$\sigma_S = \sigma_{33} \sin^2\beta + \sigma_{11} \cos^2\beta. \quad (6)$$

If the draw-direction is aligned perpendicularly to  $\vec{B}_0$  we see a doublet with the peak at

$$\sigma_{D1} = \sigma_{22}, \quad (7)$$

$$\sigma_{D2} = \sigma_{11} \sin^2\beta + \sigma_{33} \cos^2\beta. \quad (8)$$

Application of these relations for highly oriented polyethylene is shown in Ref. 2. More general expressions are derived in Ref. 3.

## Polyimide (terlon)

The structure of this highly oriented fibre is shown in Fig. 2; the spectra of the isotropic material, of stretched sample parallel ( $\parallel$ -spectrum) and perpendicular ( $\perp$ -spectrum) in respect to the magnetic field are shown in Fig. 3.

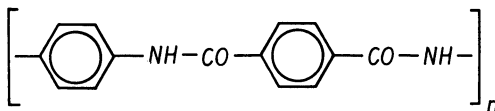


Fig. 2. Structure formula of terlon

The  $^{13}\text{C}$  nuclei neighbouring to the  $^{14}\text{N}$  do not contribute to this spectrum because of their strong broadening as a result of the dipolar interaction with the nitrogen nuclei. There are three kinds of chemically equivalent  $^{13}\text{C}$  nuclei. They are assumed to have nearly the same set of eigenvalues which can be estimated from the spectra:

$$\begin{aligned}\sigma_{11} &= -195 \pm 10 \text{ ppm (direction of C-H bonding),} \\ \sigma_{22} &= -135 \pm 5 \text{ ppm (tangential to the ring),} \\ \sigma_{33} &= 0 \pm 10 \text{ ppm (perpendicular to the ring plane);}\end{aligned}$$

( $\sigma_{33}$  was chosen for reference).

From comparison of spectra of the isotropic polymer and of the sample drawn in two directions this very important conclusion can be derived:

The draw direction lies in the plane of the phenyl rings. The proof can be given in the following manner: We will estimate angle  $\psi$  between the draw direction and the ring plane. The following conditions must be fulfilled:

- (i) The ring carbons neighbouring to the carboxylic groups cause in the  $\parallel$ -spectrum a line at the position  $\sigma_{\parallel} = \sigma_{11} \cos^2\psi + \sigma_{33} \sin^2\psi$ . In the  $\parallel$ -spectrum, there is only a signal in the range from  $\sigma_{11}$  to  $\sigma_{22}$ , leading to a possible variation of  $\psi$  from  $0^\circ$  to about  $35^\circ$ .
- (ii) In the  $\perp$ -spectrum these carbons generate a doublet. One peak is placed at  $\sigma_{\perp 1} = \sigma_{22}$ , the other at  $\sigma_{\perp 2} = \sigma_{11} \sin^2\psi + \sigma_{33} \cos^2\psi$ . Because of the absence of any peak between  $\sigma_{22}$  and  $\sigma_{33}$   $\psi$  must be  $0^\circ$  (if  $\sigma_{\perp 2} = \sigma_{33}$ ) or take a value between  $\text{ca. } 55^\circ$  and  $90^\circ$ .

Because of the contradiction of (ii) to (i) only  $\psi = 0^\circ$  is possible. With this information we can restrict the number of arrangements of greater chain units to the three possibilities shown in Fig. 4.

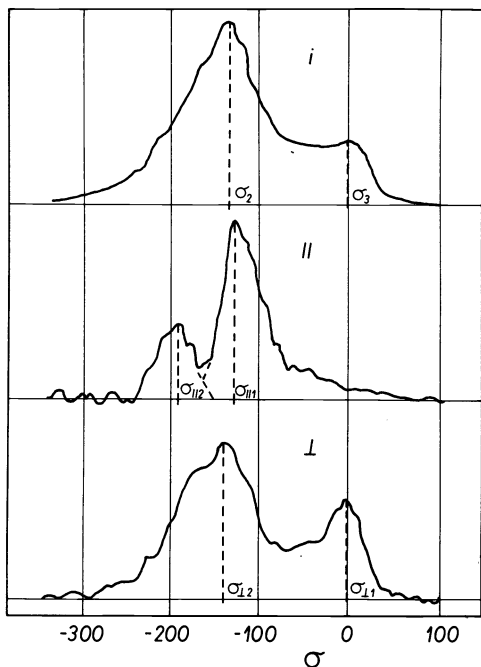


Fig. 3.  $^{13}\text{C}$  hNMR spectra of terlon (15000 scans)

- i isotropic sample
- $\parallel$  stretched sample, fibre axis parallel to  $\vec{B}_0$
- $\perp$  stretched sample, fibre axis perpendicular to  $\vec{B}_0$

Where the angles in the third case follow from the condition that the direction of the whole chain is parallel to the draw-direction. The experimental results shown in Fig. 3 cannot be explained by any of the three proposed configurations.

Structures 1 and 2 lead to lines in the  $\parallel$ -spectrum which are placed at  $\sigma_{11}$  and  $(1/4 \sigma_{11} + 3/4 \sigma_{22})$ , respectively. The right line had to be shifted by  $1/4(\sigma_{22} - \sigma_{11})$  from  $\sigma_{22}$  to lower fields. In the real  $\parallel$ -spectrum, such a shift does not occur. Moreover, structure 1 gives a ratio of intensities of 2 : 3, but we get 1 : 4 from the real spectrum.

Structure 3 yields three lines in the  $\parallel$ -spectrum at the positions

$$\sigma_{11} + 0.036 (\sigma_{22} - \sigma_{11}), \text{ relative intensity: } 1/5, \beta = 11^\circ,$$

$$\sigma_{22} + 0.570 (\sigma_{22} - \sigma_{11}), \text{ relative intensity: } 2/5, \beta = 49^\circ,$$

$$\sigma_{33} + 0.892 (\sigma_{22} - \sigma_{11}), \text{ relative intensity: } 2/5, \beta = 71^\circ.$$

Therefore, we tried to explain this by a mixture of shorter segments of the less unfavourable structures 2 and 3. For simplicity we assumed that  $\beta$  varies from  $0^\circ$  to  $11^\circ$  (and from  $60^\circ$  to  $49^\circ$  and from  $60^\circ$  to  $71^\circ$ , respectively) and every angle has equal probability. Taking into account a smoothing of the signals as a result of the dipolar interaction with the  $^{14}\text{N}$  nuclei also for  $^{13}\text{C}$  nuclei not in the immediate neighbourhood, the signal proposed for this mixture is in a good qualitative agreement with the experimental spectra.

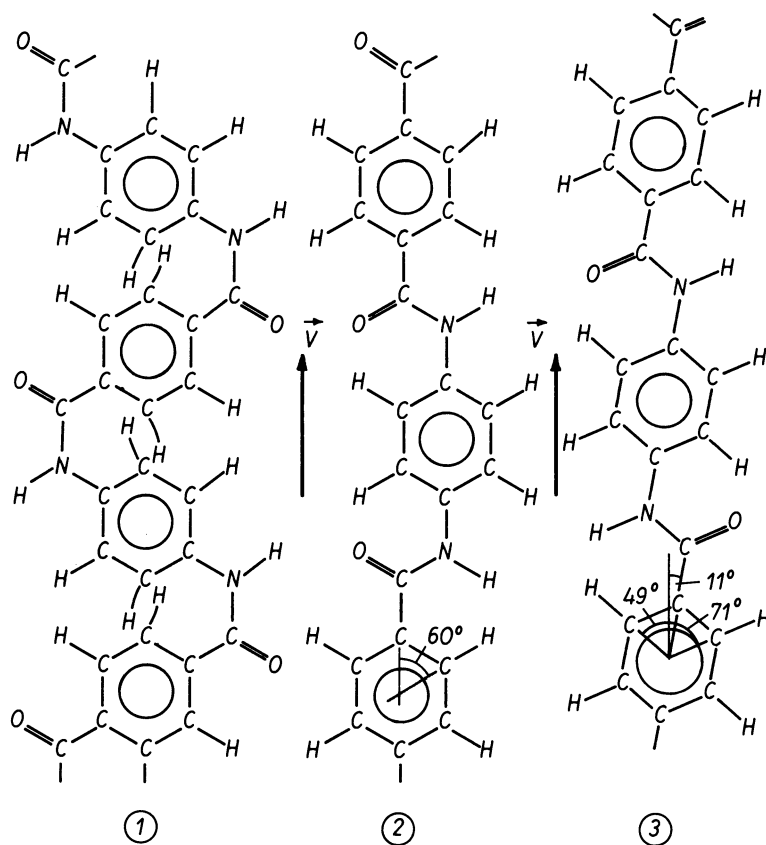


Fig. 4. Three possible arrangements of the terton chains under the assumption that the ring normals are parallel to the draw direction

For more precise conclusions according to the  $\beta$ -distribution it is necessary to use spectra with much better signal-to-noise ratio. The preparation of the sample was very complicated and the only way would be an essential increasing of the number of accumulations.

### C. WEAK ORIENTATION

Here we want to investigate into the distribution function  $k(\cos\gamma)$  of the chain segment orientations in weakly oriented polymers. Using eqn. (5) we obtain the distribution  $f(\cos\theta)$  of shielding tensor orientations from the spectra of isotropic and drawn polycarbonate, if

the tensor is axialsymmetric. However, the distribution  $k(\cos\gamma)$  of the segment orientations in respect to the draw direction is more characteristic of the polymer structure. The relations between these two directions and the principal tensor axis  $t$  are plotted in Fig. 5.

Thus, the next step must be the calculation of  $k(\cos\gamma)$  from  $f(\cos\theta)$ . From spherical trigonometry we get

$$\cos\theta = \cos\gamma \cos\alpha + \sin\gamma \sin\alpha \cos\phi \tag{9}$$

In polycarbonate  $\alpha = 90^\circ$  is well fulfilled (Fig. 6):

$$\cos\theta = \sin\gamma \cos\phi \tag{10}$$

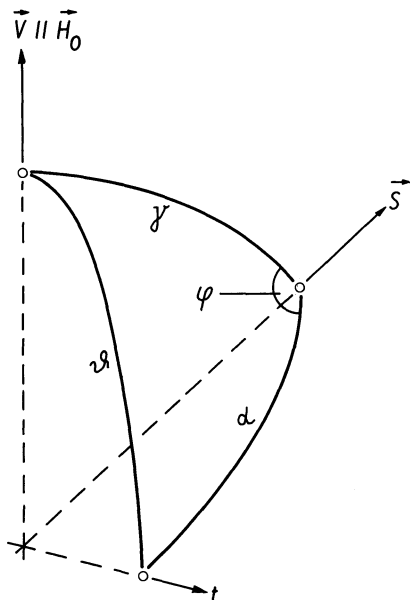


Fig.5

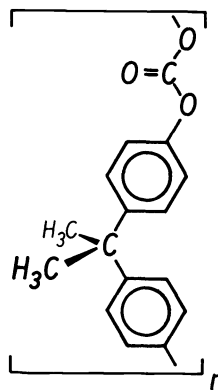


Fig.6

Fig. 5. Definition of the angles between the segment vector  $\vec{S}$ , draw-direction  $\vec{V}$ , and the tensor symmetry axis  $t$

Fig. 6. Spatial structure of polycarbonate (Ref. 4)

$\phi$  describes the rotation of a segment around this axis. We assume that all  $\phi$ 's have equal probability. If only one  $\gamma$  occurred in the sample we would find a  $\theta$ -distribution  $f_\gamma(\cos\theta)$ :

$$f_\gamma(\cos\theta) = (1/\pi) d\phi/d(\cos\theta) = (1/\pi) (\sin^2\theta - \cos^2\gamma)^{-\frac{1}{2}}. \tag{11}$$

Taking into account the distribution  $k(\cos\gamma)$  we get

$$f(\cos\theta) = (1/\pi) \int_0^{\sin\theta} k(\cos\gamma) (\sin^2\theta - \cos^2\gamma)^{-\frac{1}{2}} d(\cos\gamma). \tag{12}$$

The inversion of this integral is possible because in the integrand the upper limit occurs as a parameter. Therefore, we can calculate  $k(\cos\gamma)$  numerically step by step beginning with small values of  $\theta$ .

Polycarbonate

The spectra for the isotropic and stretched samples of polycarbonate are shown in Fig. 7. For the  $\text{CH}_3$ -line the distribution functions  $f(\cos\theta)$  and  $k(\cos\gamma)$  in Cartesian and polar coordinates calculated according to equations (5) and (12), respectively, are shown in Figs. 8 - 10.

From both Figs. 9 and 10 it can be seen that the distribution  $k(\cos\gamma)$  consists of an isotropic part (about 65%) and of a relatively highly oriented one (about 35%). The latter contains only orientations of the segments in respect to the draw-directions smaller than  $60^\circ$  with a maximum for  $\alpha = 0^\circ$ ; i.e., the polycarbonate sample stretched by a factor of 1.7 consists of two regions without and with oriented chain segments. The knowledge of the  $\gamma$ -distribution is a much more detailed information than the general integral parameter "degree of orienta-

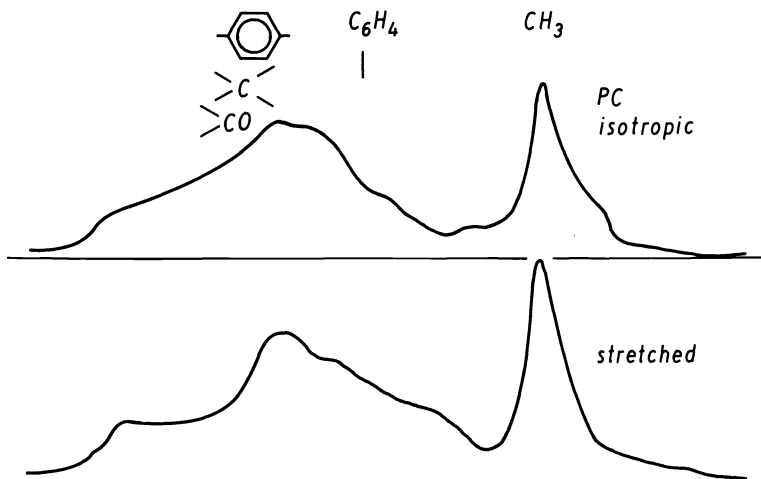


Fig. 7.  $^{13}\text{C}$  hNMR spectra of isotropic and stretched polycarbonate

tion" often determined by use of X-ray small-angle diffraction. We can give the probability for the abundance of segment orientations in a defined angle interval and - as mentioned above - eventually discuss this distribution for several regions with different orientations.

From the distribution  $k(\cos\gamma)$  we can derive also two parameters  $S_1$  and  $S_2$  which characterize the orientation degree of the sample and which are zero in the isotropic case and one in the fully oriented one.

$$S_1 = 2 \overline{\cos\gamma} - 1, \quad (13)$$

$$S_2 = \frac{1}{2}(3 \overline{\cos^2\gamma} - 1). \quad (14)$$

From the experimental results follows of course  $S_1 = S_2 = 0$  for the isotropic part;  $S_1 = 0.74$ ,  $S_2 = 0.64$  for the oriented region; and  $S_1 = 0.26$ ,  $S_2 = 0.23$  for the whole sample in good agreement with the degree of orientation determined by X-ray measurements of about 25%.

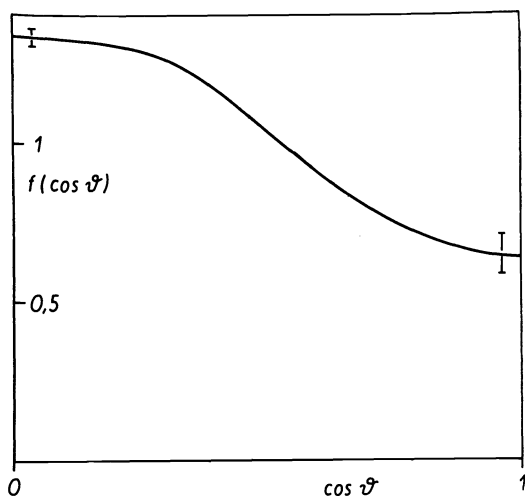


Fig. 8

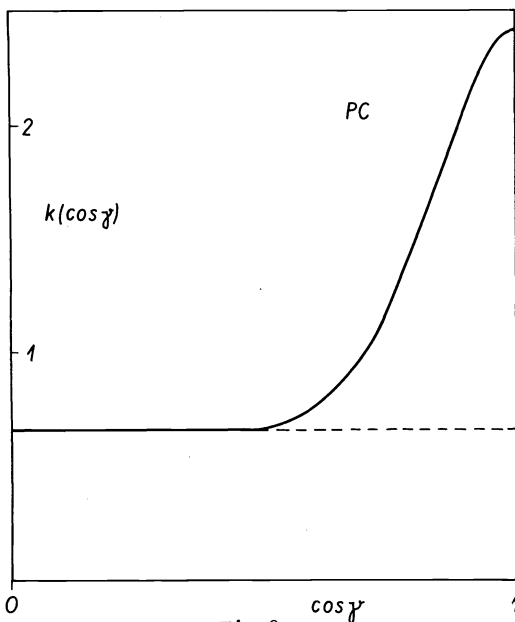


Fig.9

Fig. 8. Distribution  $f(\cos\theta)$  of the angles between the methyl symmetry axis and  $\vec{B}_0$

Fig. 9. Distribution  $k(\cos\gamma)$  between segment axis and draw-direction in Cartesian coordinates

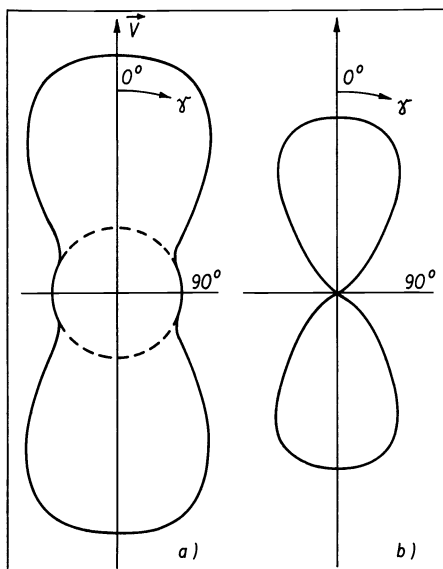


Fig. 10. Distribution  $k(\cos\gamma)$  in polar coordinates

Using  $k(\cos\gamma)$  and some statistical treatment and assuming a number of 400 segments per molecule and a length of a segment of 1.08 nm one gets for the mean length  $L_{\parallel}$  and width  $L_{\perp}$  of a polycarbonate chain in the highly ordered region

$$L_{\parallel} = 374 \text{ nm}, \quad L_{\perp} = 10.5 \text{ nm}.$$

The mean ratio of these values is 36, although the sample is stretched only by a factor of 1.7! It is hardly imaginable that this small drawing of the sample causes such a large stretching of the polymer chains.

A model, which is in a good agreement with the experimental results, assumes that these regions exist also in isotropic unstretched samples but, having their mean orientation statistically distributed, they contribute to the effect that the average orientation of the whole sample tends to zero. The stretching process then turns these "microcrystals" in the draw-direction.

### III. ISOTROPIC POLYMERS

#### A. DISTRIBUTION OF SHIELDING TENSOR ELEMENTS

Figure 11 shows two CP-spectra of high-density polyethylene with degree of crystallinity of ca. 60% and 85% respectively (estimated by X-ray scattering). (The latter sample was annealed for 6 hours at 120°C and then slowly cooled down to room temperature).

For the higher crystalline sample the spectrum becomes similar to the line shape actually occurring in a powder spectrum (Fig. 12 a).

The latter seems to be convoluted by distributions  $k_i(\sigma_{ii})$  of the shielding tensor elements  $(\sigma_{ii})$  ( $i = 1; 2; 3$ ), and the spread of these principal values is greater for the more amorphous sample. In Fig. 12 the variation of the powder spectra with general and with axial symmetry under the influence of such distributions can be seen. This phenomenon can be expressed by the relation

$$G(\sigma) = \int_{\sigma_{1l}}^{\sigma_{1u}} d\sigma_{11} \int_{\sigma_{2l}}^{\sigma_{2u}} d\sigma_{22} \int_{\sigma_{3l}}^{\sigma_{3u}} d\sigma_{33} k_1 k_2 k_3 g(\sigma; \sigma_{11}; \sigma_{22}; \sigma_{33}). \quad (15)$$

$G(\sigma)$  is the measured line shape in the spectrum,  $g$  the line shape for a theoretical powder spectrum (see e.g. Ref. 1) and  $\sigma_{il}$  and  $\sigma_{iu}$  are the lower and the upper limit of the distribution functions  $k_i(\sigma_{ii})$  of the shielding tensor elements  $\sigma_{ii}$ . From the analytical expression and also from Fig. 12 follows, that

$$g(\sigma; \sigma_{11}; \sigma_{22}; \sigma_{33}) = 0 \quad \text{if } \sigma < \sigma_{11} \quad (16)$$

( $\sigma_{11} < \sigma_{22} < \sigma_{33}$  was chosen).

Thus  $\int_{\sigma_{1l}}^{\sigma_{1u}} d\sigma_{11} \dots$  can be replaced by  $\int_{\sigma_{1l}}^{\sigma} d\sigma_{11} \dots$

if  $\sigma_{1l} < \sigma < \sigma_{1u}$ .

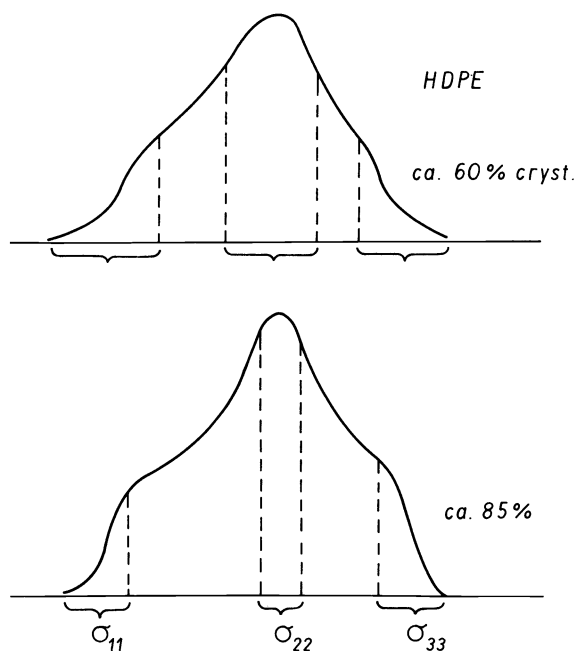


Fig. 11.  $^{13}\text{C}$  hNMR spectra of polyethylene with different degrees of crystallinity

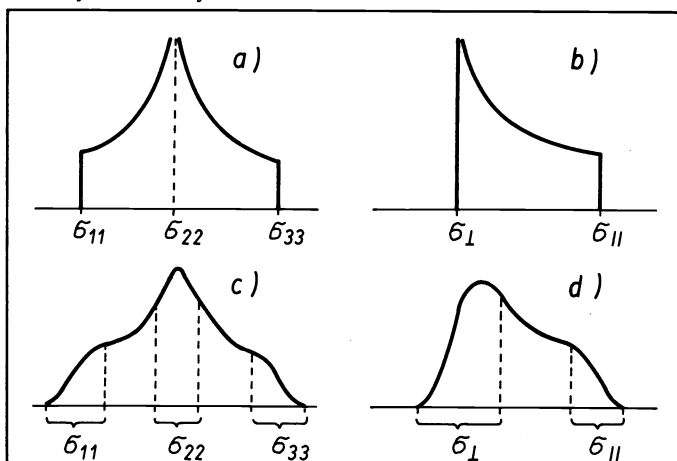


Fig. 12. Smoothing of line shape in polymers because of chemical shift distribution. (a) General symmetry, (b) axial symmetry

Under the assumption that the width of the distribution is small compared with the distance between the medians of the distributions we only use the interval  $\sigma_{1l} \leq \sigma \leq \sigma_{1u}$  (the left flank of the spectrum) for the determination of  $k_1(\sigma_{11})$ . The integrations over  $\sigma_{22}$  and  $\sigma_{33}$  yield in agreement with the mean value law of integral calculus the effective values  $\sigma_{2e}$  and  $\sigma_{3e}$  in  $g(\sigma; \sigma_{11}; \sigma_{2e}; \sigma_{3e})$ . Therefore, an integral equation with the analogous properties in respect to a parameter in the upper limit as in eq.(12) must be solved. Thus the inversion is possible. A similar treatment gives the distribution  $k_3(\sigma_{33})$ .

## B. REASONS FOR THE DISTRIBUTIONS

Many possible reasons for the distribution of shielding tensor elements were discussed in order to get information about the molecular or intermolecular structure of the polymer.

Such influences like molecular motion, residual dipolar interaction as a consequence of incomplete proton decoupling, and inhomogeneity or instability of the magnetic field can be excluded by an appropriate choice of the experimental conditions. The sum of all these effects, including the influence of the susceptibility via the geometry of the sample, is about 1 ppm and does not influence essentially the line shape. A greater contribution results from the  $^{13}\text{C} - ^{13}\text{C}$  dipolar interaction and can reach approximately 4 ppm for polymers. To reduce this influence to values smaller than 0.2 ppm an additional WHH 4 - pulse - sequence on the  $^{13}\text{C}$  frequency channel during the observation must be applied. The main reason for the  $\sigma$ -distribution is the influence of the intermolecular structure on the chemical shift of the nuclei observed. Generally, there are two ways to describe this influence:

- (i) Because of the existence of neighbouring molecules the electron cloud surrounding the observed nucleus is deformed (Van der Waals interaction), and the magnetic shielding differs from that of an isolated molecule and therefore depends on intermolecular distances. The structural disorder in amorphous regions then leads to a spread of chemical shifts. However, the latter does not exceed 1 ppm.
- (ii) The nuclei are shielded not only by their electrons but also by the polarized electron clouds of neighbouring chains or of the same chain if the distance is not too large. In solids this effect dominates the former (Ref. 6). This problem can be dealt with by the point-dipole approximation for electron clouds given by McConnell (5), which is applicable for the contribution  $\Delta\sigma_{ij}^{\pm}$  of the electron cloud  $j$  to the chemical shift of the nucleus  $i$  if the distances are not less than about 2-3 times the dimension of the clouds:

$$\Delta\sigma_{ij}^{\pm} = \sigma_{0j}^{\pm} (1/s^3) (3/2) (3\cos^2\theta_0 - 1) \quad (17)$$

Here  $\sigma_{0j}^{\pm}$  is the chemical shift of the nucleus in the centre of the electron cloud  $j$ ,  $\theta_0$  is the angle between the vector  $\vec{r}_{ij}$  and the magnetic field and  $s$  is equal to  $|\vec{r}_{ij}|/a$ .

## C. APPLICATIONS

Distribution functions for the shielding tensor elements were calculated for polycarbonate, polystyrene, polyethylene with different degrees of crystallinity (see Fig. 11), and, for comparison, hexamethylbenzene. The results are discussed with regard to the three conclusions:

- (i) The width of the distribution function is correlated with amorphousness. Figure 13 (Ref. 7) shows an excellent linear behaviour of this width versus the degree of crystallinity. If we correct these values by the contribution of the  $^{13}\text{C} - ^{13}\text{C}$  interaction, also the HMB-value lies exactly on this straightline. This tendency was to be expected, but the accuracy of the linearity is surprisingly high. However, for such a small number of examples an accident cannot be fully excluded.

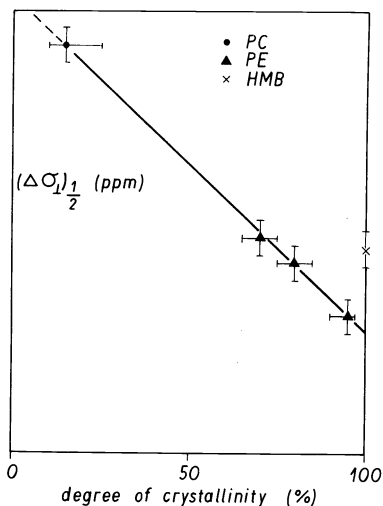


Fig. 13. Linear dependence of the width of chemical shift distribution on the crystallinity of the sample

- (ii) In all cases the distribution function calculated from the spectra can be divided into two or more parts. In Fig. 14 the shape of the methyl line (axiallysymmetric as a result of methyl rotation) in the CP spectrum of polycarbonate and the distribution functions  $k_{\perp}(\sigma_{\perp})$  and  $k_{\parallel}(\sigma_{\parallel})$  derived from that can be seen.

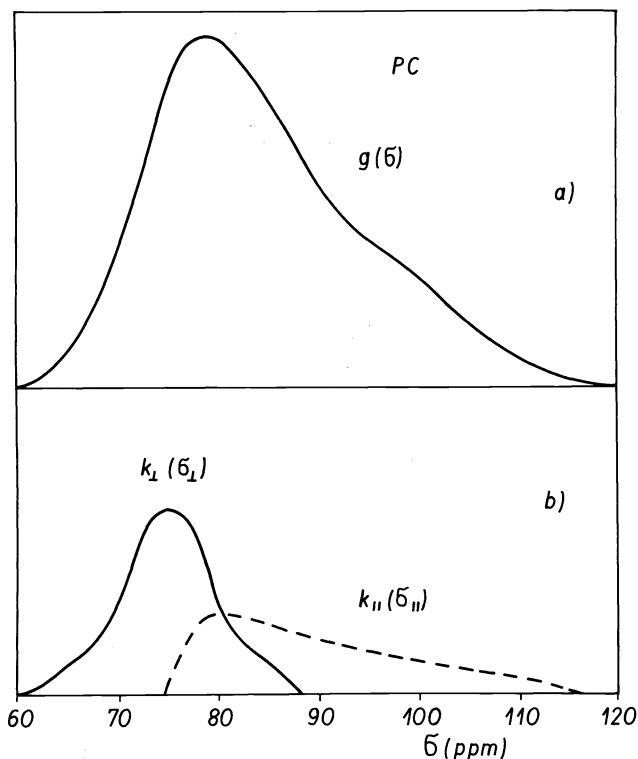


Fig. 14. Line shape and distributions of the tensorial components  $\sigma_{\parallel}$  and  $\sigma_{\perp}$  of the methyl group in polycarbonate

Two parts of Gaussian shape can be separated from  $k_{\perp}(\sigma_{\perp})$  (Fig. 15). The ratio of intensities is 3 : 1, the ratio of the widths is 2 : 1.

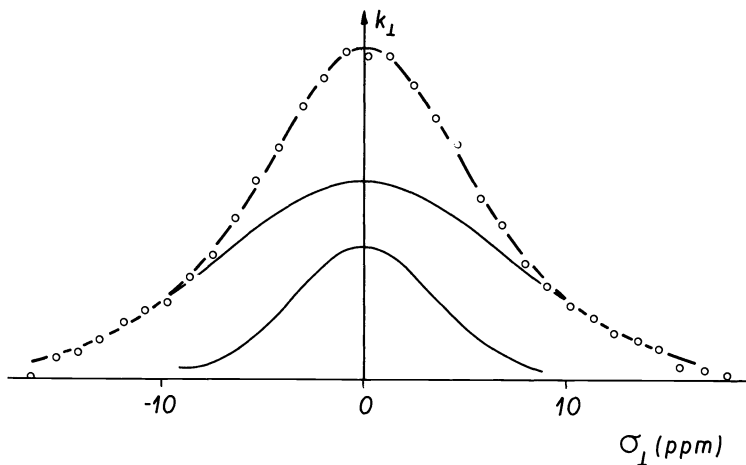


Fig. 15. Decomposition of polycarbonate  $k_{\perp}(\sigma_{\perp})$  in two Gaussian curves

Thus, two different regions exist in isotropic polycarbonate where the smaller one is more ordered. This result is in a good agreement with the model discussed in chapter II. C. for stretched polycarbonate.

- (iii) The distribution function of the shielding tensor components yields information about the conformation in the polymer chains. Equation (17) was applied to calculate the shielding tensor element distributions for polyethylene (Fig. 16).

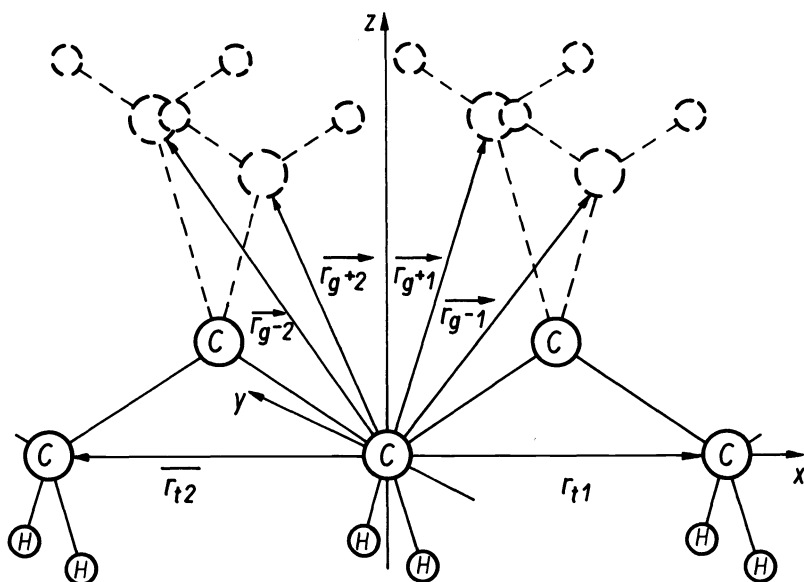


Fig. 16. Possible conformations of a methylene pentade from a polyethylene molecule.

The arrangement of four carbons is characterized by trans (t), gauche<sup>+</sup> ( $g^+$ ) and gauche<sup>-</sup> ( $g^-$ ) conformations. Thus nine conformations exist for the methylene pentade ( $tt$ ,  $tg^+$ ,  $tg^-$ , ...,  $g^-g^-$ ). Conformation changes have a much greater influence on the chemical shift than variations of the intermolecular distances. The result of the calculations shows an increase in the shielding tensor components  $\sigma_{11}$  and  $\sigma_{22}$ , but a decrease in  $\sigma_{33}$  (so that  $\text{tr}\vec{\sigma}$  is constant) in the sequence ( $g^+g^+$ ), ( $g^+g^-$ ), ( $tg^+,g^+t$ ),  $tt$ . If the probability that a conformation is trans is called  $w$ , it follows that the probabilities for  $g^+$  and for  $g^-$  are  $\frac{1}{2}(1-w)$  and for the above-mentioned sequence  $\frac{1}{4}(1-w)^2$ ,  $\frac{1}{4}(1-w)^2$ , and  $w^2$ , respectively. For a comparison with experimental data we need distribution functions which are not influenced by other interactions. Because the  $^{13}\text{C}$ - $^{13}\text{C}$  decoupling did not yet work we performed a reconvolution of the distribution function  $k_{\perp}(\sigma_{\perp\perp})$  for polyethylene by means of a Lorentzian shape with a width of the order of the additional broadening. The result is to be seen in Fig. 17.

The right part of the deconvoluted  $k_{\perp}(\sigma_{\perp\perp})$  is related to the ( $tt$ )-conformation and has an intensity of 5/6 of the whole distribution (corresponding to  $w^2$ ). That means, the probability for trans conformations  $w$  is approximately 90% and for both gauche conformations together about 10%.

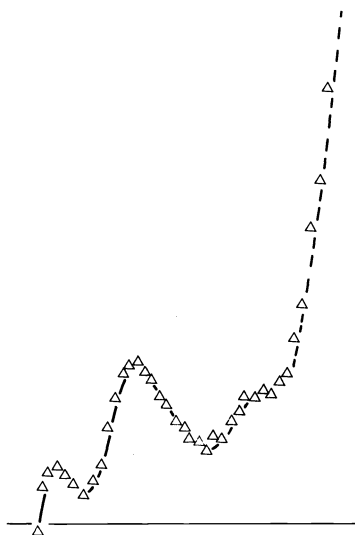


Fig. 17.  $k_{\perp}(\sigma_{\perp\perp})$  of polyethylene deconvoluted by a Lorentzian function.

## IV. CONCLUSIONS

Some possibilities for the interpretation of the line shape of cross-polarization spectra were shown. The results yield additional information for other physical and chemical measurements about the structure of solid polymers.

Especially mean orientations, distributions of orientations, degree of crystallinity and orientation, some regions with different order or orientation and conformations are discussed. Improvement of the theoretical treatment is necessary now. Although the methods are too complicated for routine measurements, the application to the study of many other polymers (in connection with nearly magic angle spinning) seems to be possible and useful.

Acknowledgement

The authors thank R. Richter and J. Fiebig for helpful discussions and experimental collaboration.

## REFERENCES

1. A. Pines, M.G. Gibby and J.S. Waugh, J. Chem. Phys. 59, 569-590 (1973)
2. S.J. Opella and J.S. Waugh, J. Chem. Phys. 66, 4919-4924 (1977)
3. G. Hempel, Thesis, Merseburg 1980
4. R. Houwink and A.I. Stavermann, Chemie und Technologie der Kunststoffe, Geest & Portig, Leipzig (1962)
5. H.M. McConnell, J. Chem. Phys. 27, 226-229 (1957)
6. U. Haeblerlen, Proc. of the XXth Coll. Spectr. Intern. Praha 1977, p. 373-383
7. J. Fiebig, Diplomarbeit, Merseburg 1979